Theoretical Study of the Activation of Alkane C–H and C–C Bonds by Different Transition Metals

Margareta R. A. Blomberg,* Per E. M. Siegbahn, Umpei Nagashima,‡ and Jan Wennerberg

Contribution from the Institute of Theoretical Physics, University of Stockholm, Vanadisvägen 9, S-11346 Stockholm, Sweden. *Received May 17, 1990*

Abstract: The activation of C–H and C–C bonds by different transition metal atoms has been studied using quantum chemical methods including electron correlation. The metals studied are iron, cobalt, nickel, rhodium, and palladium. A general result for all these metals is that the barrier for C–C insertion is found to be 14–20 kcal/mol higher than the barrier for C–H insertion. This can be explained by the difference in directionality between bonds to methyl groups and to hydrogen atoms. The size of the activation barrier is similar among transition metals in the same row but is considerably lower for the second-row metals than for the first-row metals studied here. This latter result follows from the more efficient sd-hybridization obtained for second-row metals, which in turn follows from the more similar size of the *n*d and $(n + 1)$s orbitals for these atoms. The differences in the atomic spectra between first- and second-row metals also play a part in making the barrier for second-row metals lower. Similar explanations can be used for the result that the exothermicity for the insertion reaction is larger for second-row metals and for the result that $M–R_1$ and $M–R_2$ bond energies are nearly additive in MR_1R_2 complexes of second-row metals.

I. Introduction

Alkanes are unusually stable compounds and they are also among the most abundant organic compounds in nature. The abundance of the alkanes makes them important raw materials for chemical synthesis. The stability of the alkanes, on the other hand, makes the selective transformation into other compounds difficult. Therefore, the selective activation of alkane carbon–hydrogen and carbon–carbon bonds is a challenge to organic chemists. Transition metals can activate saturated hydrocarbons, and for practical purposes mostly heterogeneous catalysts are at present employed, partly because they can operate at high temperature. The selectivity is, however, often poor in these reactions, and therefore a large effort has been put into the study of alkane activation by transition metals in homogeneous media under mild conditions. It was not until 1982 that direct intermolecular insertion of a metal center into unactivated carbon–hydrogen bonds was first observed.[1,2] These first observations involved iridium and rhodium complexes, but subsequently insertion into alkane carbon–hydrogen bonds was observed also for rhenium, iron, and osmium complexes.[3] One important question in this context which will be addressed in the present paper is whether there are any differences between the transition metals in their ability to activate saturated hydrocarbons. The analogous insertion of a metal center into unactivated carbon–carbon bonds has not yet been observed, despite the ready cleavage of carbon–carbon bonds by heterogeneous catalysts. This observation poses a second question, and this is why the C–H bond is more easily broken than the C–C bond, although the C–H bond is stronger.

Another question of general interest is to what extent metal–ligand bond energies are transferable, i.e., whether a metal ligand bond has the same strength in different compounds. In the present paper the particular question, whether a metal–R bond has the same strength in a compound with two R ligands as it has in a compound with only one R ligand, is discussed. Here R denotes a methyl group or a hydrogen atom. It is of special interest to find out if there are any general differences between first- and second-row transition metals in this context.

The experimental results for C–H activation indicate that the metal insertion into the C–H bond occurs via a concerted C–H oxidative addition pathway.[1] We have therefore chosen to study the oxidative addition of a metal atom into the carbon–carbon bond of ethane (reaction 1) and into the carbon–hydrogen bond of methane (reaction 2).

In the present study bare metal atoms are used not only because of the interest in these systems as such, but most of all as the simplest possible models of metal complexes. For the product complexes, MR_1R_2, the ground state is often a linear high-spin state, but the bent low-spin state is the best model of actual metal complexes with ligands. Thus it is this latter state that is studied here. In order to make the modelling as meaningful as possible, most of the comparisons between the different metals are further made keeping the same atomic state for all metals, the $d^{n+1}\,s^1$ state, which is the state that best models the metal in the complex before the addition of the R groups for all the metal atoms studied here, except possibly for palladium. As will be seen below, this procedure leads to much larger similarities between the different metals than what is found for the atomic ground-state gas-phase reactivities. In actual chemical reactions in solution the ligands in the metal complexes may obviously play an important role. We believe, however, that the reaction mechanisms are best understood if the inherent metal atom properties are separated from the ligand effects. In parallel to the bare metal atom studies, we have also investigated the ligand effects on the reactions.[4] Three first-row transition metals (iron, cobalt, and nickel) and two second-row transition metals (rhodium and palladium) are studied in the present paper. Of these, only iron and rhodium are known to insert into carbon–hydrogen bonds in homogeneous media. Both reaction energies and barrier heights are calculated.

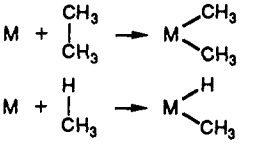

(1)

(2)

The question concerning differences in the carbon–hydrogen and the carbon–carbon activation mechanisms has been addressed previously in model calculations. In a study comparing alkane activation to the activation of molecular hydrogen,[5,6] we found that the alkane activation reactions have higher barriers than the hydrogen activation reaction. This difference was explained by

‡Current address: Institute for Molecular Science, Okazaki, Japan.

(1) (a) Janowicz, A. H.; Bergman, R. G. *J. Am. Chem. Soc.* **1982**, *104*, 352. (b) Janowicz, A. H.; Bergman, R. G. *J. Am. Chem. Soc.* **1983**, *105*, 3929.

(2) Jones, W. D.; Feher, F. J. *J. Am. Chem. Soc.* **1982**, *104*, 4240.

(3) *Perspectives in the Selective Activation of C-H and C-C Bonds in Saturated Hydrocarbons*; Meunier, B., Chaudret, B., Ed.; Scientific Affairs Division-NATO: Brussels, 1988.

(4) Blomberg, M. R. A.; Schüle, J.; Siegbahn, P. E. M. *J. Am. Chem. Soc.* **1989**, *111*, 6156.

(5) Blomberg, M.; Brandemark, U.; Pettersson, L.; Siegbahn, P. *Int. J. Quantum Chem.* **1983**, *23*, 855.

(6) Blomberg, M. R. A.; Brandemark, U.; Siegbahn, P. E. M. *J. Am. Chem. Soc.* **1983**, *105*, 5557.

0002-7863/91/1513-424$02.50/0

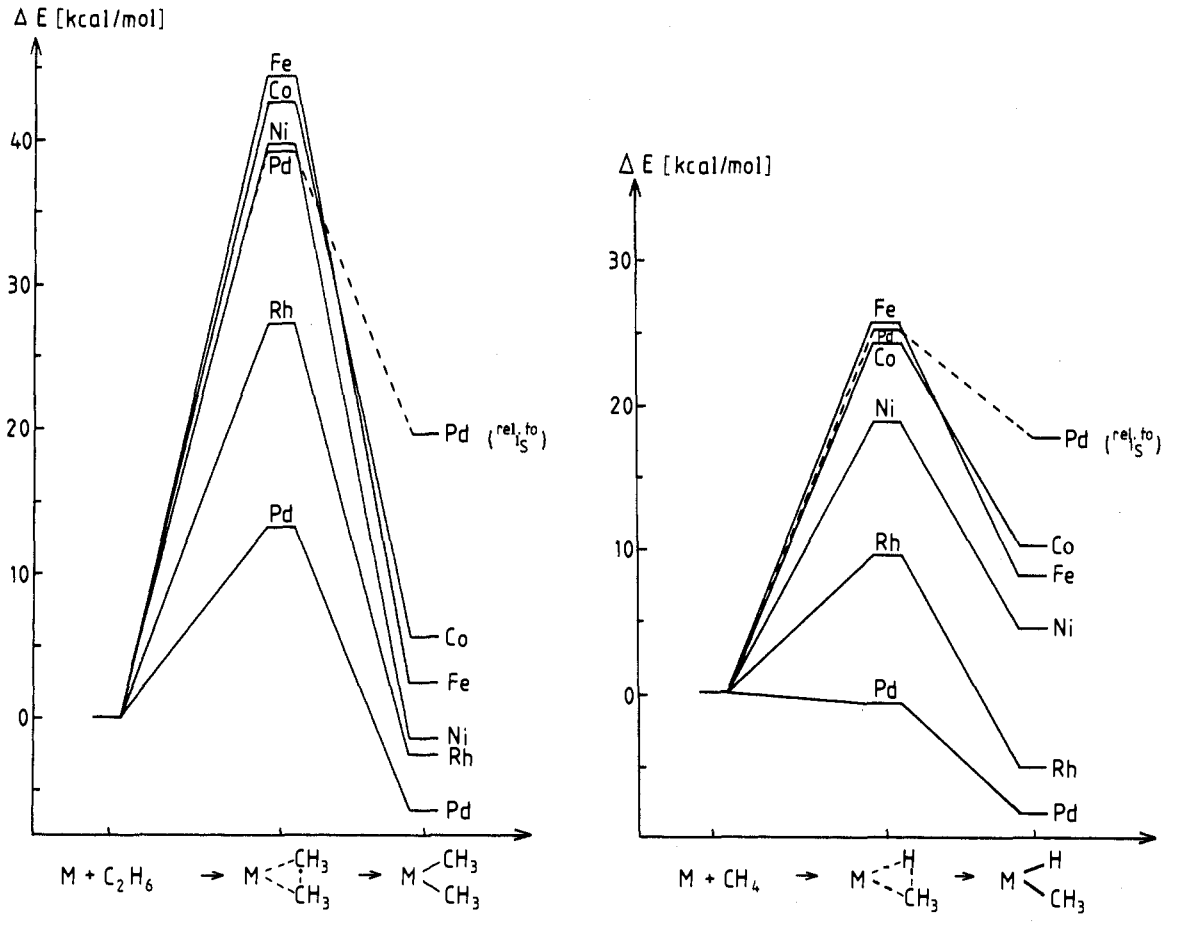

Figure 1. Calculated (CCI + Q) reaction energies and activation energies for reactions 1 and 2. The low-spin d^{n+1} s state of the metals is used as dissociation limit. For palladium the energies relative to the ground state $^1S(d^{10})$ (dashed curve) are also given.

the directed nature of the methyl group compared to the spherical nature of the hydrogen atom. This directionality makes it energetically more unfavorable for methyl groups than for hydrogen atoms to bind both to the metal and the other R group in the transition-state structure. Thus, a C–C activation barrier of 42 kcal/mol was obtained in that study,[6] compared to 3 kcal/mol for the H–H activation barrier. Using this proposed mechanism, we further predicted that the C–H activation barrier should lie somewhwere between the C–C activation and the H–H activation barriers.[5] This difference in barrier heights would be in line with the experimentally observed difference in reactivity between C–H bonds and C–C bonds. However, this prediction about the C–H barrier height was not confirmed by the subsequent calculations in ref 6, where in fact a somewhat higher barrier was obtained for the C–H activation compared to the C–C activation, a result that seemed to contradict the proposed reaction mechanism. As it turns out, the reason for this surprising result is simply that the calculations on the nickel insertion into methane suffered from a computational problem which eventually led to an unbalanced description of the different parts of the potential surface. The new, more accurate, results obtained in the present study give a substantially lower barrier for the C–H activation by nickel. In the meantime, the correct order between the C–H and C–C activation barriers was obtained by Low and Goddard[7a,b] in a study on the palladium and platinum reactions with ethane and methane, where, for example, the barrier height for C–H activation by palladium was calculated to be 30 kcal/mol, compared to 39 kcal/mol for the C–C activation.

Most of the calculations reported in the present paper are performed at a standard level, i.e., using medium-sized basis sets and correlating the electrons involved in bond breaking and bond formation, plus the valence d electrons on the metal. The complete active space self-consistent field (CASSCF) approach is used to include near-degeneracy effects in the wave functions, and the multireference externally contracted configuration interaction (CCI) method is used to include dynamical correlation effects. However, at a later stage of the calculations it was decided that the accuracy of the results should be investigated further, and more accurate calculations were performed on some selected systems. In these calculations large primitive basis sets with polarization functions were used on all atoms, and all valence electrons, including the valence electrons on the R groups, were correlated. In this case the internally contracted average coupled pair functional (IC-ACPF) method was used to calculate size consistent correlation energies. The main result from these larger benchmark calculations is that the smaller standard treatment is adequate for answering the more general chemical questions mentioned above, but for quantitative predictions the more accurate treatment is needed. The methods used are further described in the Appendix, together with basis sets, geometries, electronic states, etc.

II. Comparison between Different Metals

In this section comparisons will be made between different transition metal atoms with respect to their ability to activate the C–C bond in ethane (reaction 1) and the C–H bond in methane (reaction 2). Reaction energies and activation energies for the two reactions are calculated and the results are given in Table I and are also shown in Figure 1. The $d^{n+1}s^1$ state (low spin coupled, to keep the spin conserved) is used as the dissociation limit for all atoms except palladium where results with respect to the d^{10} state are also given. The main result for the first-row metal atoms is that they have very similar reaction energies and reaction barriers. For the second-row metals, the insertion reactions are more exothermic than for the first-row metals, and the reaction barriers are lower. The results for the reaction

(7) (a) Low, J. J.; Goddard, W. A., III *J. Am. Chem. Soc.* **1984**, *106*, 8321. (b) Low, J. J.; Goddard, W. A., III *Organometallics* **1986**, *5*, 609. (c) Low, J. J.; Goddard, W. A., III *J. Am. Chem. Soc.* **1984**, *106*, 6928. (d) Low, J. J.; Goddard, W. A., III *J. Am. Chem. Soc.* **1986**, *108*, 6115.

Table I. Calculated (CCI + Q) Relative Energies (in kcal/mol) for Insertion of the Metal Atom into the C–C Bond of C_2H_6 and into the C–H Bond of CH_4[a]

	Fe		Co		Ni		Rh		Pd	
	C_2H_6 $^3B_2$	CH_4 $^3A'$	C_2H_6 $^2A_1$	CH_4 $^2A'$	C_2H_6 $^1A_1$	CH_4 $^1A'$	C_2H_6 $^2A_1$	CH_4 $^2A'$	C_2H_6 $^1A_1$	CH_4 $^1A'$
ΔE	+2.4	+7.9	+5.3	+10.0	−1.5	+4.3	−2.6	−6.3	−6.3 (+19.7)	−8.4 (+17.6)
ΔE^* (add)	+44.5	+25.5	+42.7	+24.1	+39.8	+19.8	+27.3	+9.4	+13.2 (+39.2)	−0.9 (+25.1)
ΔE^* (elim)	+42.1	+17.6	+37.4	+14.1	+41.3	+15.5	+29.9	+15.7	+19.5	+7.5

[a] The energies are given relative to the low-spin $d^{n+1}s$ state of the free metal atom. For palladium the energies relative to the ground state $^1S(4d^{10})$ are also given (within parentheses). Positive values for the reaction energies, ΔE, means that the addition reaction is endothermic. ΔE^*(add) is the barrier for the addition reaction and ΔE^*(elim) is the barrier for the elimination reaction.

energies are discussed in section A below and for the activation energies in section B. In section C comparisons are made to the metal atom insertion reaction into the hydrogen molecule. The accuracy of the results is discussed in section V.

A. Reaction Energies. The reaction energies for the different metals investigated are rather similar. For the C–C insertion the reaction energies vary between −6.3 kcal/mol (for Pd) and +5.3 kcal/mol (for Co), and for the C–H insertion between −8.4 kcal/mol (for Pd) and +10.0 kcal/mol (for Co). There are, furthermore, large similarities between the C–C and the C–H insertion reactions. For each metal the difference in exothermicity (or endothermicity) of the two reactions is less than 6 kcal/mol. Also, if the metals are ordered after the magnitude of the reaction energies, the order is the same for the two reactions. The largest difference obtained for the reaction energies is the larger exothermicity of the second-row metals compared to the first-row metals. For the C–H bond cleavage the reaction energy varies between −8.4 and −6.3 kcal/mol for the second-row atoms and between +4.3 and +10.0 kcal/mol for the first-row atoms. For the C–C bond cleavage the difference between the rows is smaller, with the reaction energies varying between −6.3 and −2.6 kcal/mol for the second row and between −1.5 and +5.3 kcal/mol for the first row. For the H–H bond cleavage in H_2 (see below), the difference between the two rows is larger than that for both the C–C and the C–H bond cleavage. There is thus a tendency for larger differences between the rows when bonds to hydrogen are involved in the reaction. The origin of this tendency is a combination of the fact that an R group added as a second ligand binds much better to a second-row atom than to a first-row atom (see further below) and that the hydrogen atom binds stronger than the methyl group to transition metals.

The result for the relative strength of the first- and second-row MR_1R_2 binding energies is in agreement with the experimental finding that oxidative addition adducts are more stable for second-row metals than for first-row metals.[8] The experimental results further show that the third-row metals form the most stable MR_1R_2 compounds. The larger MR_1R_2 binding energies for the second-row metals compared to the first-row metals can be explained along two lines, one related to the relative radial extension of the metal orbitals and the other to the spectra of the metal atoms. When only one R ligand binds to the metal, the M–R bond is formed by the valence s electron on the metal, and it is expected that the first- and second-row transition metals should form M–R bonds of roughly the same strength (when the same atomic state is used as reference point). This expectation is supported by calculated M–R binding energies; see, for example, ref 9. The difference in MR_1R_2 binding energies between the rows therefore has to be found mainly in the second M–R bond. With two R ligands the $d^{n+1}s$ state of the metal is the main binding state; i.e., the two covalent bonds are formed by two sd hybrids on the metal. Thus the strength of the second M–R bond is determined by the possibility to simultaneously form strong bonds to a metal s and a metal d electron. It is, therefore, expected that the second bond in the MR_1R_2 compound is stronger if the s and d orbitals on the metal have more similar density maxima. For the second-row transition metals the 4d and 5s orbitals have maxima closer to each other than the 3d and 4s orbitals of the first-row metals. For rhodium and palladium, for example, the ratio between the radii of maximum charge density of the 4d and 5s orbitals is about 0.40, whereas for cobalt and nickel the corresponding ratio is only 0.27.[10]

Table II. Metal Populations at Minima and Transition-State Structures (CCI Results)

	Fe		Co		Ni	
	C_2H_6 $^3B_2$	CH_4 $^3A'$	C_2H_6 $^2A_1$	CH_4 $^2A'$	C_2H_6 $^1A_1$	CH_4 $^1A'$
minimum						
3d	6.57	6.64	7.75	7.84	8.75	8.81
4s	0.74	0.76	0.56	0.55	0.64	0.71
4p	0.24	0.21	0.23	0.23	0.20	0.20
transition state						
3d	6.48	6.48	7.67	7.63	8.84	8.82
4s	0.92	0.99	0.94	1.02	0.88	0.91
4p	0.45	0.42	0.35	0.33	0.26	0.26
	Rh		Pd			
	C_2H_6 $^2A_1$	CH_4 $^2A'$	C_2H_6 $^1A_1$	CH_4 $^1A'$		
minimum						
4d	8.17	8.25	9.20	9.23		
5s	0.35	0.40	0.45	0.48		
5p	0.12	0.11	0.20	0.16		
transition state						
4d	8.44	8.42	9.56	9.50		
5s	0.20	0.32	0.22	0.30		
5p	0.11	0.11	0.13	0.13		

Further, the differences in the atomic spectra between the first- and second-row metals also contribute to the stabilization of the second-row complexes compared to the first-row complexes. The atomic state of the metal in the MR_1R_2 complex is not a pure $d^{n+1}s$ state, but rather a mixture between this state and other low-lying states. For the first-row metals, the states that are lower or similar in energy to the $d^{n+1}s$ state have a d^ns^2 occupation, while for the second-row metals it is the d^{n+2} state that is the other low-lying state. From Table II, where the Mulliken populations for the metals are given, it can be seen that for the first-row metals the 3d populations are smaller than $n + 1$ at the minima (i.e., the d^ns^2 state is mixed in), while for the second-row metals the 4d populations are larger than $n + 1$ (i.e., the d^{n+2} state is mixed in). It is expected that the additional s electron in the d^ns^2 state introduces a larger repulsion toward the R groups than the d^{n+2} state, and thus the second-row metals obtain larger MR_1R_2 binding energies than the first-row metals.

For palladium the reaction energies for the insertion reactions are markedly different if the $^1S(4d^{10})$ state is used as dissociation limit rather than the $^1D(4d^95s^1)$ state. Reactions 1 and 2 change from being exothermic by 6.3 and 8.4 kcal/mol, respectively, using the $^1D(4d^95s^1)$ dissociation limit, to being endothermic by 19.7 and 17.6 kcal/mol, respectively, using the $^1S(4d^{10})$ dissociation limit. In the latter case the $M(CH_3)_2$ and $MHCH_3$ binding energies are thus smaller for palladium than for all the other metals.

(8) Jones, W. D. Working paper for NATO workshop on *Selective Activation of C-H and C-C Bonds in Saturated Hydrocarbons*; Strasbourg, 1988.
(9) Bauschlicher, C. W., Jr.; Langhoff, S. R.; Partridge, H.; Barnes, L. A. *J. Chem. Phys.* **1989**, *91*, 2399.
(10) Fraga, S.; Karwowski, J.; Saxena, K. M. S. *Handbook of Atomic Data*; Elsevier: Amsterdam, 1976.

Table III. Calculated (CCI + Q) Relative Energies (in kcal/mol) for Insertion of the Metal Atom into the H_2 Molecule[a]

	Fe $^3B_1$	CO $^2A_1$	Ni $^1A_1$	Rh $^2A_1$	Pd $^1A_1$
ΔE	−0.7[b]	−2.6[b]	−8.0[b]	−31.2	−34.1 (−8.1)

[a] The energies are given relative to the low-spin $d^{n+1}s$ state of the free metal atom. For palladium the energies relative to the ground state $^1S(4d^{10})$ are also given (within parentheses). [b] From ref 11 and 12; relativistic effects are not included.

B. Activation Energies. The calculated activation energies are very similar for the first-row metal atoms, and the order of the metals is the same for the C–C and the C–H insertion. Also for the second-row metal atoms the activation energies are reasonably similar. Between the two rows there are, however, rather large differences with the second-row metals having markedly lower barriers than the first-row metals. For the C–C insertion the activation energies vary from +13.2 kcal/mol (for Pd) to +44.5 kcal/mol (for Fe), and for the C–H insertion from −0.9 kcal/mol (for Pd) to +25.5 kcal/mol (for Fe). The most important result for the activation energies is the difference between the C–C activation and the C–H activation, which will be discussed further in section III below. For all the metals the difference in activation energy between the two reactions is the same; the C–C activation has a barrier 14–20 kcal/mol larger than the C–H activation.

The lower reaction barriers obtained for the second-row metals follow the result for the reaction energies. The larger binding energies for the second-row MR_1R_2 complexes give rise to lower barriers for reactions 1 and 2. One of the mechanisms suggested above to lower the energy of the second-row MR_1R_2 complexes, the involvement of the d^{n+2} state, is even more pronounced at the transition state as can be seen from the population analysis in Table II. For the second-row metals the d population is increased at the transition state, compared to the minimum MR_1R_2 structure (i.e., the involvement of the d^{n+2} state is increased), while for the first-row metals there is a slight tendency to decrease the d population, (i.e., to increase the involvement of the more repulsive d^ns^2 state). The change in d population is largest for palladium, which is caused by the low-lying d^{n+2} (d^{10}) state of the palladium atom. Since this state is actually the ground state, this leads to significantly lower barriers for palladium than for rhodium when the d^{n+1} s state is used as reference point. Using the d^{10} state as reference for the palladium reactions gives a barrier of 39.2 kcal/mol for the ethane insertion and 25.1 kcal/mol for the methane insertion, while going to a d^9s reference decreases the barriers to 13.2 kcal/mol and −0.9 kcal/mol, respectively. It can be noted that the former values are rather close to the values for the first-row metals.

C. Comparison to H–H Activation. The similarities between metal–CH_3 and metal–H bonding make it interesting to compare reactions 1 and 2 to the metal insertion into the hydrogen molecule. This reaction occurs with very low or no barrier,[11] a fact that will be further discussed in section III below in connection with the comparison between C–H and C–C activation. In this section we will only compare the reaction energies for the H–H insertion to those of reactions 1 and 2. For this purpose our previously calculated reaction energies for the metal insertion into the H_2 molecule for the first-row metals[11,12] are summarized in Table III. It should be noted that these values do not include relativistic corrections, which are expected to increase the exothermicity of the reactions by about 3 kcal/mol (see further section VI below). To complete the comparisons the reaction energies for rhodium and palladium insertion into the H–H bond have also been calculated; these results are also given in Table III. In accordance with the ethane and methane insertion reactions, the reaction energies are given relative to the low-spin d^{n+1} s state of the metal.

The metal insertion into the hydrogen molecule is calculated to be somewhat more exothermic than the ethane and methane reactions. For the first-row metals the reactions are exothermic by about 4 to 11 kcal/mol (when approximate relativistic energies are added), and for the second-row metals by 31.2 to 34.1 kcal/mol when the d^{n+1} s state is used as reference point. As for the ethane and methane reactions, the second-row metals are more exothermic than the first-row metals, and the difference between the rows is even larger for the H–H insertion. As discussed above, the difference between the first- and second-row metals increases in the sequence C–C, C–H, and H–H activation. The difference thus increases with the number of H ligands in the MR_1R_2 complex.

III. Comparison between C–H and C–C Activation

The intermolecular oxidative addition of transition metals to alkane C–H bonds is observed in homogeneous media, while the corresponding reaction for unactivated C–C bonds has not been observed. The barrier for the C–C insertion is also calculated to be 14–20 kcal/mol higher than that for the C–H insertion for all the metals investigated here, in agreement with these observations. It is clear from the preceding section that the difference between the two reactions cannot be explained by differences in the reaction energies. In fact, the calculated reaction energies for the metal insertion are not very different for the two reactions, and, in particular, they are not in favor of the C–H insertion. The C–C insertion is slightly more exothermic than the C–H insertion for both the first- and second-row metals for the larger calculations presented in section V below. Instead, the difference between the two reactions can be explained by the reaction mechanism to be discussed below. This reaction mechanism has been discussed before,[5-7] and what is new in the present study compared to previous results is that all metals fit into the same pattern, i.e., give the same difference between the C–C and C–H activation barriers.

For the first-row metal atoms (see Table I and Figure 1), the activation energy for the C–C insertion is 40–45 kcal/mol and for the C–H insertion 20–25 kcal/mol. The second-row metals have substantially lower barriers than the first-row metals (using the d^{n+1} s dissociation limit), 13–27 kcal/mol for the C–C insertion and 0–9 kcal/mol for the C–H insertion. However, the difference between the C–H and C–C activation barriers is the same, 14–20 kcal/mol, for the first- and the second-row metals.

The fact that the difference in barrier height for the C–H insertion and the C–C insertion is so constant from metal to metal supports the previously suggested mechanism involving the difference in directionality between the H and the CH_3 bond.[5,6] Since the spherically symmetrical hydrogen atoms can bind to the metal atom and to each other at the same time in the transition-state structure, the metal insertion into the H_2 molecule forming the bent MH_2 complex has a very low or no barrier.[11] The sp^3-hybridized carbon in a methyl group, on the other hand, has one optimal binding direction, and when the metal–carbon bond is starting to form in the MR_1R_2 complex the methyl groups have to rotate into a position that is no longer optimal for the R_1–R_2 bond. This gives rise to a higher barrier for metal insertion into C–C and C–H bonds compared to the H–H bond, and also to a higher barrier for the insertion into a C–C bond compared to the insertion into a C–H bond, since in the first case two methyl groups are involved and in the latter case only one. Since this mechanism mainly involves the R_1–R_2 binding, it also makes it very likely that the difference in barrier height between reactions 1 and 2 should be quite independent of the metal.

Previous results for palladium and platinum reactions[7] agree qualitatively with the presently obtained results for the difference between C–H and C–C activation and thus already supported the suggested reaction mechanism. However, for the nickel insertion into the C–H bond of methane the presently obtained results are qualitatively different from the previous results in ref 6, which suffered from a computational problem, making the relative energies of different parts of the potential surface unbalanced. The most important difference is that the reaction barrier has decreased from 54 kcal/mol in ref 6 to the present value of 20 kcal/mol,

(11) (a) Blomberg, M. R. A.; Siegbahn, P. E. M. *J. Chem. Phys.* **1983**, *78*, 986. (b) Blomberg, M. R. A.; Siegbahn, P. E. M. *J. Chem. Phys.* **1983**, *78*, 5682.

(12) Siegbahn, P. E. M.; Blomberg, M. R. A.; Bauschlicher, C. W., Jr. *J. Chem. Phys.* **1984**, *81*, 1373.

Table IV. Additivity of M–CH_3 and M–H Binding Energies in MR_1R_2 Complexes[a]

	Co		Ni		Rh	
	$\Delta E(MR_1R_2)$	$\Delta E(MR_1) + \Delta E(MR_2)$	$\Delta E(MR_1R_2)$	$\Delta E(MR_1) + \Delta E(MR_2)$	$\Delta E(MR_1R_2)$	$\Delta E(MR_1) + \Delta E(MR_2)$
$R_1 = R_2 = CH_3$	62.6	88.6	71.9	87.0	65.6	64.6
$R_1 = H; R_2 = CH_3$	83.6	107.5	91.8	111.3	94.4	94.1
$R_1 = R_2 = H$	99.9	126.4	108.1	135.6	120.5	123.6

[a] $\Delta E(MR_1R_2)$ is the calculated reaction energy $MR_1R_2 \rightarrow M + R_1 + R_2$, and $\Delta E(MR_i)$ is the calculated reaction energy $MR_i \rightarrow M + R_i$. The values are given in kcal/mol and all values are given relative to the high-spin $d^{n+1}s$ state of the free metal atom. CCI+Q results.

making the C–H activation energy lower than the C–C activation energy. Thus, the new calculated activation energies for nickel insertion into the C–H and C–C bonds also support the suggested reaction mechanism.

Considering the reverse reactions, the elimination of ethane and methane from the MR_1R_2 complexes, the following should be noted. First, as can be seen in Table I, the C–H coupling has a lower barrier than the C–C coupling for all the metals. This result, of course, is explained by the same reaction mechanisms as discussed above for the addition reactions. In ref 7b it was actually concluded, based on the results for palladium and platinum, that the barrier height for the C–C coupling is twice that for the C–H coupling. The present study does not support such a general relationship and, in particular, does not give a ratio of 2 for the palladium reactions. Our results presented in Table I give a ratio larger than 2 for the activation energies of C–C and C–H coupling for most of the metals, and, further, our most accurate calculations, to be discussed below, indicate that the ratios for the barrier heights vary considerably between the metals. For palladium our most accurate value for the ratio of the activation energies is about 4, and for nickel it is close to 2. Secondly, previous calculations show that processes involving H–H bonds have essentially no barriers, owing to the spherical nature of the H atoms as discussed above. From this fact, it should not be concluded, however, that the H–H coupling occurs more easily than the C–H and C–C couplings. For palladium, for example, the dihydride is bound relative to the ^1S ground state of palladium by about 8 kcal/mol, and the activation barrier for C–H coupling is 7.5 kcal/mol in our standard calculation. Thus, about the same activation energy is needed for H–H coupling and C–H coupling.

IV. Transferability of M–R Bond Energies

An interesting general question is to what extent metal–R binding energies can be transferred from one system to another. If metal–R bonds have the same strength in different complexes, this would clearly mean a dramatically improved possibility to make predictions, since the thermochemistry of chemical reactions involving the formation or breaking of metal–R bonds could be simply obtained using known experimental or theoretical data from other complexes. In the present paper we investigate whether the first and the second metal–R bond have the same binding energy; i.e., we question whether the MR_1R_2 binding energies are equal to the sum of the $M–R_1$ and $M–R_2$ binding energies. To answer this question the M–R binding energies for some selected metals have been computed at the same level as for the MR_1R_2 compounds. In Table IV the sum of the $M–R_1$ and $M–R_2$ binding energies are given together with the MR_1R_2 binding energies calculated relative to the $M + R_1 + R_2$ limit. The results for the metal insertion into the H_2 molecule are also included in this table. For all these energies the high-spin $d^{n+1}s$ state is used as reference point for the metal atom. For cobalt this leads to larger binding energies than if the ground d^ns^2 state is used as reference point. As can be seen from Table IV, for the first-row metals cobalt and nickel the MR_1R_2 binding energy is substantially smaller (by 15–27 kcal/mol) than the sum of the $M–R_1$ and $M–R_2$ binding energies, while for the second-row metal rhodium, the corresponding values are very close to each other. Thus, for second-row metals M–R binding energies seem to be transferable, but not so for the first-row metals. The explanation for this difference between the first- and second-row metals is the following. In the M–R compound the bond is mainly formed by the valence s electron in the metal $d^{n+1}s$ state, while in the MR_1R_2 compound the two bonds are formed from sd hybrids on the metal. For the first-row the second bond becomes weaker because of the difference in radial maxima for the 4s and 3d orbitals as discussed above, while for the second-row metals the second bond is of similar strength to the first one.

The conclusion about nontransferability of M–R binding energies for the first-row metal atoms is confirmed by the larger calculations on the nickel complexes, using larger basis sets and correlating all valence electrons (see section V). The absolute binding energies are larger in the more accurate calculations but the deviation from additivity of the M–R bond energies is almost identical with the corresponding results of the standard calculations. As can be seen from Table IV, the $Ni(CH_3)_2$ binding energy is 15.1 kcal/mol smaller than twice the $NiCH_3$ binding energy, and the $NiHCH_3$ binding energy is 19.5 kcal/mol smaller than the sum of the NiH and $NiCH_3$ binding energies in the standard calculation. The corresponding numbers for the more accurate calculations are 16.2 and 20.0 kcal/mol, respectively.

V. Accuracy of the Calculations

In this paper we have focused on general and qualitative chemical questions and partly adapted our computational approach to this goal. However, it is our definite experience that, even if only qualitative results are needed to answer the chemical questions, this still puts rather high demands on the methods and basis sets used. For example, in the nickel case the results for the thermochemistry of reactions 1 and 2 are changed from the Hartree–Fock value by 50–60 kcal/mol by the inclusion of near-degeneracy and dynamical correlation effects in the calculations. Simple calculations at the Hartree–Fock level will thus not at all be enough for a study of this type of reactions. Even though the present standard calculations do include electron correlation, one can still ask whether the calculations performed are accurate enough, since the basis sets lack, for example, d functions on carbon and f functions on the metals and since not all the valence electrons have been correlated (the inactive CH bond electrons are not correlated). We show below that our results are indeed accurate enough for comparing different metals and different reactions, but if absolute values for reaction energies and activation energies are required larger calculations have to be performed.

To investigate the accuracy of the standard calculations we have performed large benchmark calculations for the nickel and palladium reactions. We have used large basis sets and have correlated all valence electrons using the internally contracted multireference average coupled pair functional method. The details are further described in the Appendix. The results from these calculations are in Table V and Figure 2 compared to the results from the standard calculations. In this comparison we use the $^1S(4d^{10})$ dissociation limit for palladium. As can be seen, the exothermicity of the reactions is increased by 8–12 kcal/mol, and the barriers are lowered by 2–10 kcal/mol compared to the standard calculations. However, the differences between the two metals are changed by less than 3 kcal/mol for both reaction energies and activation energies. Also for the comparison of the two reactions, the C–H activation and the C–C activation, the large calculations agree with the standard calculations. The standard calculations give for each metal rather similar reaction energies for the two reactions and further, for all metals, a difference in barrier height for the C–C and the C–H activation in the range 14–20 kcal/mol. The large calculations give the same results on these two points. We therefore conclude that the results

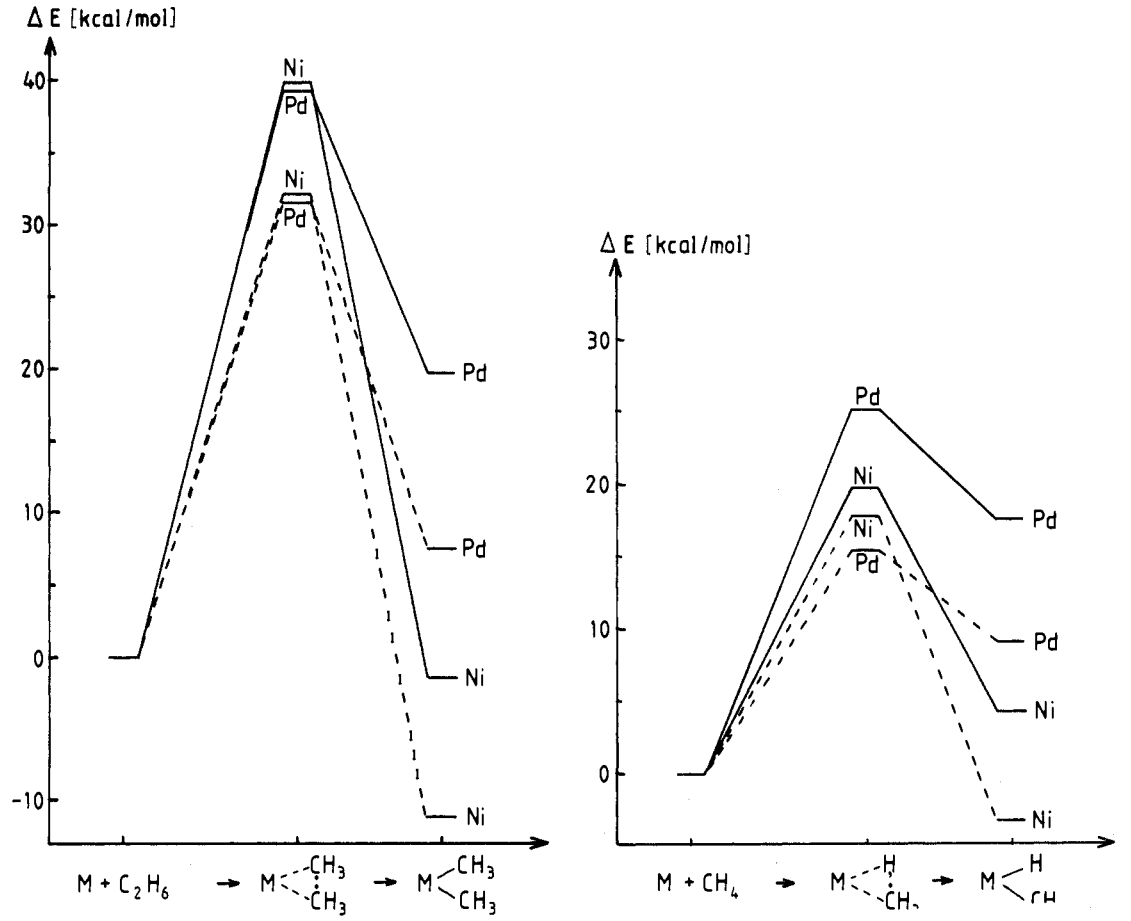

Figure 2. Calculated reaction energies and activation energies for reactions 1 and 2 for nickel and palladium. The full lines are the results from the standard calculations (CCI + Q) and the dashed lines the results from the larger calculations, using larger basis sets and correlating all valence electrons (IC-ACPF). The reference point used is for nickel the $^1D(d^9\,s)$ state and for palladium the $^1S(d^{10})$ state.

Table V. Comparison between the Large (IC-ACPF, Large Basis, CH Correlation) and the Standard (CCI + Q, Standard Basis, No CH Correlation) Calculations for the Insertion of Nickel and Palladium into the C-C Bond of C_2H_6 and into the C-H Bond of CH_4[a]

	Ni			
	C_2H_6		CH_4	
	large	standard	large	standard
ΔE	-11.1	-1.5	-3.3	+4.3
ΔE^*(add)	+32.1	+39.8	+17.9	+19.8
ΔE^*(elim)	+43.2	+41.3	+21.2	+15.5
	Pd			
	C_2H_6		CH_4	
	large	standard	large	standard
ΔE	+7.5	+19.7	+9.1	+17.6
ΔE^*(add)	+31.5	+39.2	+15.4	+25.1
ΔE^*(elim)	+24.0	+19.5	+6.3	+7.5
ΔE[b]	+16.0		+20.1	
ΔE^*(add)[b]	+38.6		+30.5	
ΔE^*(elim)[b]	+22.6		+10.4	

[a] The relative energies (in kcal/mol) are for nickel given relative to the $^1D(3d^9 4s)$ state and for palladium relative to the ground state $^1S(4d^{10})$. Positive values for the reaction energies, ΔE, means that the addition reaction is endothermic. ΔE^*(add) is the barrier for the addition reaction and ΔE^*(elim) is the barrier for the elimination reaction. [b] Low and Goddard.[7b]

presented in Table I and Figure 1 are accurate enough for making the comparisons done in the previous sections.

The thermochemistry of reactions 1 and 2 depends on the strength of the metal-R bonds but also on the C-C binding energy of ethane and the C-H binding energy of methane, respectively. Thus the accuracy of the calculated relative energies depends on the accuracy of the description of all these bonds. An estimate of the accuracy of the calculated C-C binding energy of ethane and C-H binding energy of methane can be obtained by comparing experimental values. The experimental value for the C-C bond is 99 kcal/mol and for the C-H bond 111 kcal/mol. These values are obtained by subtracting the zero-point energies from the measured values in order to enable comparison with our calculated values. The C-C bond energy is increased by 14.4 kcal/mol, from 77.9 to 92.3 kcal/mol in going from the standard calculations to the large calculations. For the C-H bond an increase of the binding energy of 5.7 kcal/mol is obtained, from 103.6 to 109.3 kcal/mol. The results from the large calculations are thus reasonably close to the experimental values. The increase in binding energies has two sources, the improved basis sets and the correlation of the inactive CH electrons. The improvement of the basis set increases the C-C bond energy by 10.2 kcal/mol and the C-H bond energy by 3.7 kcal/mol. The remaining bond energy increases of 4.2 kcal/mol for C-C and 2.0 kcal/mol for C-H originate from the correlation of the inactive CH bonding electrons. Thus the correlation of the inactive CH electrons contributes 2 kcal/mol per methyl group involved in the bonding.

As discussed above, the insertion reactions 1 and 2 become more exothermic in going from the standard calculations to the large calculations. Thus the increase in C-C and C-H binding energies described in the preceding paragraph is more than counterbalanced by the increased metal-R binding energies. The basis set improvements also change the atomic spectra of the metals, which will also influence the relative energies. The comparisons made below for the reaction energies are made using the d^{n+1} s atomic dissociation limit for both nickel and palladium. The $^1D(4d^9 5s)$ limit for palladium gives an exothermicity of the ethane insertion reaction of 23.0 kcal/mol and for the methane insertion of 21.4 kcal/mol.

The effects on the reaction energies of reactions 1 and 2 from introducing correlation of the inactive CH electrons are quite independent of the metal involved. Correlation of the CH electrons increases the exothermicity of the ethane insertion reaction by 7.7 kcal/mol for nickel and 8.1 kcal/mol for palladium. The corresponding numbers for the methane insertion reaction are 3.4 kcal/mol for nickel and 3.8 kcal/mol for palladium. Thus, the effect of CH correlation on the MR_1R_2 binding energies relative to $M + R_1R_2$ is an increase of the binding energy by about 3–4 kcal/mol per methyl group involved. This means that the effect of CH correlation is 3–4 kcal/mol larger on the methyl-to-metal bonding than on the methyl-to-methyl or methyl-to-hydrogen bonding.

The effects on the reaction energies from increasing the basis sets, on the other hand, are rather different for the two metals investigated. For the nickel reaction with ethane, the improvement of the C–C bond of ethane is larger than the improvement of the Ni–C bonds, leading to a decrease of the exothermicity of reaction 1 by about 4 kcal/mol when the standard basis set is replaced by the larger basis set. For the nickel reaction with methane, the basis set improvement decreases the endothermicity by about 1 kcal/mol. If just a single d function on carbon is added to the standard basis set, results very similar to those for the large basis set are obtained for the nickel reaction energies and also for the C–C and the C–H bond energies. These results show that the f functions on nickel give a very small contribution to the bonding.

For the palladium reactions the improvement of the metal–C and metal–H bonding is much larger than for nickel, leading to an increase of the exothermicity of both the ethane and methane reactions by 7–8 kcal/mol when the large basis set is used. This result indicates that the f functions are more important on palladium than on nickel, which is partly due to the higher valence d population on palladium at the minimum structure, around 9.2 for palladium compared to 8.7–8.8 for nickel. The importance of f functions on palladium can also be due to the stronger d-bonding in the PdR_1R_2 complexes compared to the NiR_1R_2 complexes. This difference in basis set dependence between nickel and palladium is expected to be a general difference between first- and second-row metals, since second-row metals generally have higher d populations (compare Table II) and stronger d-bonding than first-row metals.

VI. Relativistic Effects

As described in the Appendix we have used first-order perturbation calculations to obtain relativistic contributions to the energies. We thus obtain both nonrelativistic and relativistic energies, and we can therefore determine the effect of relativity on the relative energies. First, it should be mentioned that the relativistic effects are quite independent of the level of calculation, i.e., very similar for correlated and uncorrelated wave functions. For the first-row metals the relativistic effect is quite constant from metal to metal and also for the different states studied. The relative energies at minima and transition states are lowered by 2–4 kcal/mol for both the ethane and the methane insertion reactions for all these metals. This energy lowering could be interpreted as a result of the involvement of the $d^n s^2$ state at the minima and transition-state structures, since the $d^n s^2$ state has a larger relativistic energy than the d^{n+1} s state used as dissociation limit. This interpretation is, however, too simplified, since the larger relativistic energy of the $d^n s^2$ state compared to the d^{n+1} s state is caused by the larger 4s population, and as can be seen from Table II the 4s populations in the complexes are smaller than one (at the minima) or equal to one (at the transition states). This indicates that it is the formation of covalent bonds to the transition metal that causes at least part of the large relativistic contribution to the energy at minima and transition states. A similar interpretation can be made of the relativistic effects on the bond energy in the gold dimer.[13] For the second-row metals the effects of relativity are larger; the binding energies are increased by 6–10 kcal/mol. Further, also the results for the second-row metals indicate that the relativistic effects on the relative energies are not only due to the relativistic effects on the splitting between the atomic states. As discussed in section IIA, the metal configuration in these complexes is a mixture of the d^{n+1} s and d^{n+2} atomic states. Since the d^{n+1} s state, used as dissociation limit, has a larger relativistic energy than the d^{n+2} state, the mixture of the two states in the complexes should lead to a decrease of binding energy due to relativity. Contrary to this expectation, the binding energies are actually increased by relativity, and again the covalent bonds to the metal in the complex should be responsible for at least part of the increased relativistic contribution to the energy. For the transition-state structures of the palladium complexes, relativity causes a slight increase of the barrier heights, by 1–4 kcal/mol, and, as can be seen from Table II, the 4d population is here larger than at the minimum, and apparently so large that the effect from the involvement of the $4d^{10}$ state dominates.

If the $4d^{n+2}$ state is used as dissociation limit for the second-row metals, the relativistic effects on the relative energies become much larger. The binding energies are increased by 20–22 kcal/mol by relativity for the palladium complexes and by 17–21 kcal/mol for the rhodium complexes. The relativistic effect on the binding energies is thus larger than the relativistic effect on the $4d^{n+2}$ to $4d^{n+1}5s$ splitting of the metal atoms, which is about 15 kcal/mol for palladium and about 14 kcal/mol for rhodium. This result is also in line with the interpretation that covalent bonds to the transition metal increase the relativistic contribution to the energy. At the transition-state structures the relativistic effect is smaller, 10–14 kcal/mol, which is due to the larger involvement of the $4d^{n+2}$ state at the transition state than at the minima.

VII. Comparison to Previous Results

Low and Goddard[7a,b] performed generalized valence-bond configuration interaction (GVB-RCI) calculations on the palladium and platinum atomic insertion into the C–C bond of ethane, the C–H bond of methane, and molecular hydrogen. Their results for the ethane and methane reactions are included in Table V. They used relativistic effective core potentials for the metals and essentially valence double-ζ atomic basis sets. They optimized the geometries for the minima and the transition states. In our calculations we have used their geometries for the palladium reactions. For the case of the ethane and methane reactions with palladium, our results using the smaller standard treatment and their results are quite similar, both for reaction energies and activation energies. However, the rather large effect on the absolute values of these energies we obtain from going to the larger more accurate treatment should be noted. Our most accurate estimate of the barrier for insertion of the palladium atom into the C–H bond, for example, is only about half of that obtained by Low and Goddard, 15.4 kcal/mol compared to 30.5 kcal/mol, relative to the ^1S state. Considering the elimination reactions, the results obtained by Low and Goddard is that the C–C coupling has an activation barrier that is twice the C–H activation barrier, while our most accurate calculations give a ratio of about 4 for the palladium reactions. For the PdH_2 binding energy, already the discrepancy between our standard treatment and the results of Low and Goddard is quite large. In our calculations, PdH_2 is bound relative to H_2 and $Pd(^1S)$ by 8.1 kcal/mol, while they obtained a negative binding energy of 3.6 kcal/mol.

For the nickel insertion into ethane and methane our results from the standard calculations in the present paper can be compared to our previous results from ref 6. For the ethane reaction the results are quite similar, even though the binding energy has increased by almost 7 kcal/mol, which is mainly a result of the reoptimization of the geometry. However, as discussed in section III, for the methane reaction the results are qualitatively different, indicating serious errors in the previous calculations. Most important, the reaction barrier has decreased from 54 kcal/mol in ref 6 to the present value of 20 kcal/mol, making the C–H activation energy lower than the C–C activation energy, in agreement with the predictions based on the proposed reaction mechanisms.[5] Also the binding energy has increased, making $NiHCH_3$ unbound

(13) Schwerdtfeger, P.; Dolg, M.; Schwarz, W. H. E.; Bowmaker, G. A.; Boyd, P. D. W. *J. Chem. Phys.* **1989**, *91*, 1762.

by only 4 kcal/mol in the present calculations, compared to 21 kcal/mol in ref 6. The reason for the large changes of the energetics for the nickel insertion into methane is that the old calculations were suffering from a technical error, making the description of different parts of the potential surface unbalanced.

VIII. Conclusions

The first striking result of the present study is that the difference in activation barrier between a C–H and a C–C insertion is the same, 14–20 kcal/mol, for all the metal atoms. This result points toward a difference in the mechanism between the two reactions which is also independent of the metal atom. Such a mechanism was indeed suggested many years ago[5] and simply involves the difference in directionality of a bond to a methyl group and to a hydrogen atom. A hydrogen atom can bind to the other R group and to the transition metal at the same time, whereas the methyl group has to tilt in the process of breaking (or forming) the R_1–R_2 bond. This leads to a predicted order of the barriers for the R_1–R_2 insertion which is lowest for H–H and highest for C–C and with C–H in-between. This result agrees with available experimental evidence.

The results of the present calculations give a rather simple picture of the electronic mechanism for oxidative addition and its reverse, reductive elimination. The first conclusion is that it is the d^{n+1} s state which is active in breaking the R_1–R_2 bond. To obtain a low barrier for the addition reaction the d^{n+1} s state has to be a low-lying state, preferrably the ground state. Then, since one s bond and one d-bond will be formed in the addition process, sd-hybridization has to be efficient. Efficient hybridization requires orbitals of similar size, and the addition reaction therefore proceeds much easier for metal atoms in the second transition row than for those in the first row. In contrast to the case of the addition reaction, a low barrier for the elimination reaction also depends on the relative energies of the reactants and products. Therefore, a large binding energy as for the case of RhH_2 can lead to a high elimination barrier.

In the entrance channel of the addition reaction where the stable closed-shell R_1R_2 molecule approaches the metal atom, the avoidance of repulsion is important for obtaining a low barrier. To avoid repulsion several different state mixings with resulting orbital hybridizations can take place. If there is a low-lying d^n s^2 state, an sp-hybridization away from the alkane is going to be important. This is the dominating hybridization in the entrance channel for iron and cobalt since the d^n s^2 state is much lower than the other states for these atoms. For nickel, the dominating initial hybridization is of sd_σ type,[6] which should not be confused with the sd-hybridization required to form the final two bonds in the complex. In the sd_σ-hybridization a plus-combination of s and d_σ will point toward the alkane and be strongly repulsive, whereas the minus-combination will point perpendicular to the line connecting the alkane and the transition metal and will thus be much less repulsive. Moving electrons from sd_+ to sd_- will thus decrease the repulsion without changing the total d and s occupations. sd_σ-hybridization requires a state where s and d_σ are singlet coupled. For transition metals of the first row the singlet–triplet splitting for the d^{n+1} s occupation is much smaller than for the second-row metals, which will partly compensate for the fact that hybridization is more difficult between orbitals of very different size as in the first row. This type of hybridization is the dominating one in the bonding between nickel and carbonyl but is important also in the earlier stages of the alkane addition reaction. The third type of state mixing which is important in the entrance channel involves moving the repulsive s electrons down into the d shell by using the d^{n+2} state. This mixing is particularly important and efficient for second-row metals since the d^{n+2} state is a low-lying state (the ground state for palladium) but can also be seen to some extent to the right in the first row.

As mentioned in the Introduction, of the metals studied here only iron and rhodium have been shown experimentally to insert into C–H bonds. For the rhodium insertion into methane a barrier of 9.4 kcal/mol was calculated at the standard level. However, considering the effects obtained for nickel and palladium from increasing the accuracy of the calculations, it is likely that the addition barrier will more or less disappear if the calculations for the rhodium–methane reaction are improved and agreement with the experimental observation would thus be obtained. For iron, on the other hand, a rather high barrier of 17.6 kcal/mol was obtained in the calculations, and in this context it should be noted that the model calculations already employ a state of the iron atom that is excited by about 35 kcal/mol above the ground state. Therefore, very large ligand effects are needed in the iron case to explain the experimental observation that iron insertion into the C–H bond actually occurs.

The final conclusion which will be drawn from the present results is that even though the individual energies will be quite sensitive to the details of the wave function, relative energies can be usefully obtained at a standard level of treatment provided electron correlation is reasonably well included. To obtain quantitatively accurate reaction energies, the correlation of all the valance electrons of the system cannot be avoided, neither can the inclusion of f functions on the metal. For example, the barrier for inserting a palladium atom into methane was in a previous study found to be 30.5 kcal/mol using a standard treatment,[7a,b] but in the present most accurate calculations a barrier of only 15.4 kcal/mol was obtained.

Appendix: Computational Details

A. Geometries. For each metal the energies were calculated at three points on the potential surfaces of reactions 1 and 2: the separated systems M + R_1R_2, a bent MR_1R_2 structure representing the product minima, and an intermediate structure representing the transition states. The important geometric parameters used are given in Figure 3. For all first-row metals the nickel geometries in Figure 3a–d were used. For the second-row metals the palladium geometries in Figure 3e–h were used, except for the rhodium reaction with methane where the geometries given in Figure 3i,j were used. Calculations on the iron reaction with methane yielded relative energy differences smaller than 1.5 kcal/mol between the nickel optimized geometries and corresponding geometries optimized for iron, for both the minimum and the transition state. It was therefore concluded that only minor effects on the potential surfaces would be obtained from full geometry optimizations for each metal, and the above-described geometries were therefore used. For ethane, methane, and the methyl radical the experimental geometries were used. For PdH_2 and RhH_2 the geometry optimized for PdH_2 in ref 7b was used.

B. Electronic States. For metals with more than one hole in the d shell, the most optimal orbital occupation of MR_1R_2 gives rise to many different electronic states, and all these possible states have been studied. These states are the $^2A_1$, $^2B_1$, and $^2A_2$ states for the cobalt and rhodium reactions with ethane, the $^2A'$ and $^2A''$ states for the cobalt and rhodium reactions with methane, the $^3A_1$, $^3B_2$, $^3B_1$, and $^3A_2$ states for the iron reaction with ethane, and the $^3A'$ and $^3A''$ states for the iron reaction with methane. For each metal, all states give very similar relative energies for each of the reactions 1 and 2, with only one exception. The exception is the $^3A_1$ state of $Fe(CH_3)_2$, which has a higher barrier and a lower binding energy than the other states. For each of the studied reactions results are reported for only one of the possible states. Totally symmetric states were chosen in all cases except for the iron reaction with ethane for which the $^3B_2$ state was chosen.

C. Methods. The complete active space SCF (CASSCF) method[15] was used to include the near-degeneracy effects in the wave functions. The active space was chosen to include the two metal–R_1R_2 bonding orbitals. For the first-row metals one doubly occupied totally symmetric d orbital was also included since this orbital is mixed with the valence s orbital on the metal to form an sd hybrid. Two weakly occupied orbitals are further included in the active space. One of these can be characterized as the antibonding orbital correlating the totally symmetric bonding orbital (binding mainly with s on the metal) as well as the other

(14) Koga, N.; Morokuma, K., private communication.
(15) Roos, B. O.; Taylor, P. R.; Siegbahn, P. E. M. *Chem. Phys.* **1980**, *48*, 157.

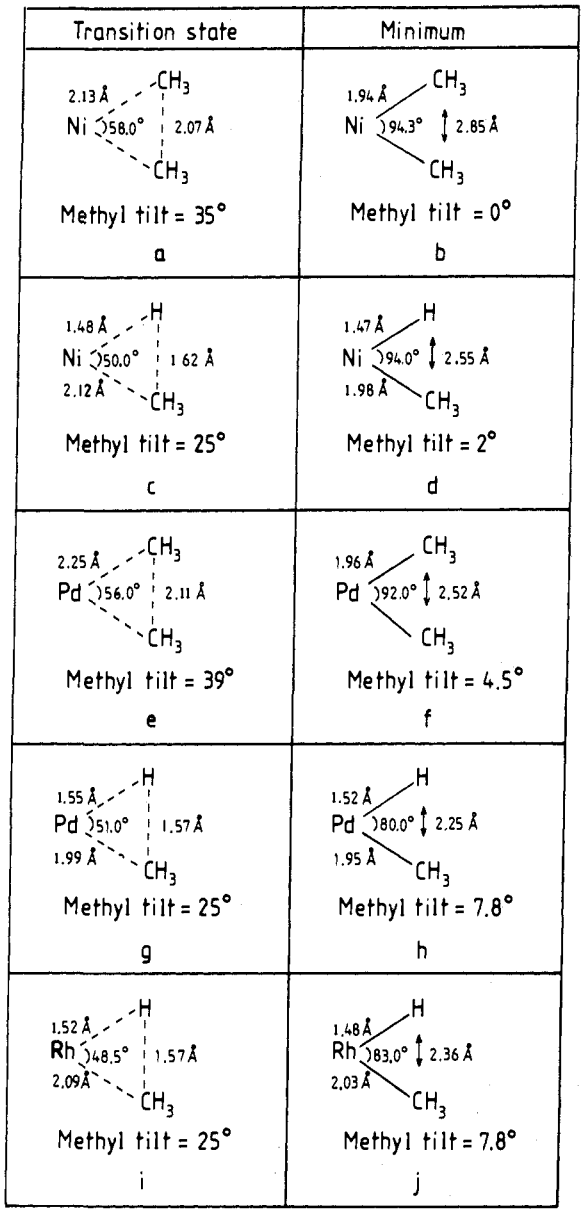

Figure 3. Transition state and minimum geometries. The geometries in a–d are taken from ref 6 except for the minimum structure of $Ni(CH_3)_2$ (b), which was partly reoptimized in the present study. The geometries in e–h are taken from Low and Goddard.[7] The geometries in i and j are taken from ref 14 and were optimized for the $RhCl(PH_3)_2$ reaction with methane. For the latter structures no value for the methyl group tilt angle was given, and this was therefore taken from the palladium structures.

component of the sd hybrid (for the first-row metals). The other weakly occupied orbital is the antisymmetric antibonding orbital. At the dissociation limit the C–C or C–H bonding orbital to be broken was active, together with an antibonding orbital.

The most important configuration at the minimum, besides the Hartree–Fock configuration, is the excitation from the bonding orbital formed by the d orbital on the metal to the corresponding antibonding orbital. At the transition-state structure the situation differs markedly between the first- and second-row metals. For the second-row metals, excitations from the two bonding orbitals are approximately equally important at the transition-state structures. For the first-row metals, however, the most important excitations at the transition state are excitations from a totally symmetric spd-hybridized orbital pointing away from the R ligands, which is doubly occupied in the Hartree–Fock configuration, to the orthogonal spd-hybridized orbital pointing toward the R ligands, which is empty in the Hartree–Fock configuration. These excitations are most important for iron and decrease somewhat going to the right in the periodic system.

Table VI. Hartree–Fock Splittings (eV) for the Two Lowest States of the Metal Atoms Using the Standard Basis Sets

atom	lower state	upper state	ΔE_{SCF} nonrelativistic	NHF[a]	ΔE_{SCF} relativistic	HFR[a]
Fe	$^5D(d^6s^2)$	$^5F(d^7s)$	1.85	1.80	2.05	2.06
Co	$^4F(d^7s^2)$	$^4F(d^8s)$	1.50	1.53	1.82	1.83
Ni	$^3D(d^9s)$	$^3F(d^8s^2)$	−1.28	−1.27	−1.54	−1.63
Rh	$^4F(d^8s)$	$^2D(d^9)$	0.91	0.95	1.47	1.54
Pd	$^1S(d^{10})$	$^3D(d^9s)$	0.74	0.75	0.11	0.10

[a] Reference 30.

Two sets of correlation calculations were performed based on the molecular orbitals from the CASSCF calculations. Using the smaller basis set, multireference externally contracted CI (CCI) calculations[16] were performed. In these calculations all configurations with a coefficient larger than 0.05 in the CASSCF wave function were chosen as reference states. On the metal the valence d and s electrons were correlated, ranging from 8 electrons on iron to 10 electrons on nickel and palladium. In the R_1–R_2 molecule only the 2 electrons in the R_1–R_2 bond to be broken were correlated, i.e., the C–C bond in ethane and one of the C–H bonds in methane. For all the CCI results reported here, the Davidson correction[17] is included (denoted CCI + Q) to account for higher than double excitations.

Using the large basis set, internally contracted average coupled pair functional (IC-ACPF) calculations[18] were performed using the same reference wave function as for the CCI calculations, but correlating also the inactive CH bonding electrons; i.e., all valence electrons were correlated. The number of correlated electrons in these calculations range between 16 and 24 electrons, and the wave functions thus obtained comprise up to about half a million configuration state functions.

The relativistic contribution to the energies is obtained by means of first-order perturbation theory where the mass–velocity and the Darwin terms are retained in the perturbation operator.[19] It has been shown in ref 20 for NiH that relativistic results for energies using perturbation theory are very similar to those obtained using a variational (no pair) method. One advantage of the perturbation approach is that both nonrelativistic and relativistic energies are obtained in the same calculation, and the size of the relativistic effects can then be assessed. For the main discussion only the results including relativistic effects are used, but in section VI the effects of relativity on the results are discussed.

D. Basis Sets. Two different basis sets were used, and these are referred to as the standard basis set and the large basis set. Mostly the generalized contraction scheme was used, either of Raffenetti type[21] for the standard sets or of ANO (atomic natural orbitals) type[22] for the large sets. The standard basis sets are described first. For the first-row metals Wachters (14s, 9p, 5d) primitive basis[23] was used, augmented with a diffuse d function and two 4p functions leading to a (14s, 11p, 6d) primitive basis. The Raffenetti contraction scheme[21] gives minimal basis in the core and double-ζ in the valence shells. The addition of the diffuse d function on the metals leads to triple-ζ description of the d shell. The contracted basis sets thus: [5s, 4p, 3d]. For the second-row metals the Huzinaga (17s, 11p, 8d) primitive basis[24] was used, augmented with one diffuse d function and two p functions in the 5p region, yielding a (17s, 13p, 9d) primitive basis. These basis

(16) Siegbahn, P. E. M. *Int. J. Quantum Chem.* **1983**, *23*, 1869.
(17) Davidson, E. R. In *The World of Quantum Chemistry*; Daudel, R., Pullman, B., Eds.; Reidel: Dordrecht, 1974.
(18) Program written by Per Siegbahn, based on the ACPF method by: Gdanitz, R. J.; Ahlrichs, R. *Chem. Phys. Lett.* **1988**, *143*, 413; and the internal contraction by Werner, H.-J.; Knowles, P. J. *J. Chem. Phys.* **1988**, *89*, 5803.
(19) Martin, R. L. *J. Phys. Chem.* **1983**, *87*, 750. See also: Cowan, R. D.; Griffin, D. C. *J. Opt. Soc. Am.* **1976**, *66*, 1010.
(20) Marian, C. M.; Blomberg, M. R. A.; Siegbahn, P. E. M. *J. Chem. Phys.* **1989**, *91*, 3589.
(21) Raffenetti, R. C. *J. Chem. Phys.* **1973**, *58*, 4452.
(22) Almlöf, J.; Taylor, P. R. *J. Chem. Phys.* **1987**, *86*, 4070.
(23) Wachters, A. J. H. *J. Chem. Phys.* **1970**, *52*, 1033.
(24) Huzinaga, S. *J. Chem. Phys.* **1977**, *66*, 4245.

sets were contracted using the Raffenetti scheme in a similar way as for the first-row metals. For the second-row metals, however, the core orbitals 4s and 4p have to be described by a double-ζ basis to reproduce the relativistic effects,[25] leading to a [7s, 6p, 4d] contraction. For palladium one extra contracted s function and one extra contracted p function was added in the 3s and 3p regions, respectively, leading to a [8s, 7p, 4d] contraction. In Table VI the splittings between the lowest atomic states of the metals are given, calculated at the Hartree-Fock level. It can be seen that the basis sets used here give results close to the Hartree-Fock limit. For carbon the primitive (9s, 5p) basis by Huzinaga[26] was used, contracted according to the Raffenetti scheme to [3s, 2p]. In some calculations one d function with exponent 0.63 was added on carbon. For the active hydrogen the primitive (5s) basis from ref 26 was used, augmented with one p function with exponent 0.8 and contracted to [3s, 1p]. The inactive methyl hydrogens were described by the (4s) basis from ref 26 contracted to [2s] and with the exponents scaled by a factor 1.2.

In the large basis set calculations a primitive (20s, 15p, 10d, 6f) basis was used for nickel,[27] ANO contracted to [7s, 6p, 4d, 2f]. This basis set gives a nonrelativistic splitting between the $^3D(d^9s)$ and the $^3F(d^8s^2)$ states of the nickel atom of -0.11 eV, correlating the 10 valence electrons in a one-reference scheme. It turned out that the ANO contracted basis set on nickel did not give reasonable relativistic energies, and the relativistic contributions to the energies for the nickel reactions were therefore taken from the calculations using the standard basis set. The relativistic effect on the ^3D to ^3F splitting of the nickel atom is -0.26 eV using the standard basis set, yielding an estimated splitting for the large basis of -0.37 eV, compared to the experimental value of 0.03 eV. For palladium the primitive Huzinaga basis[24] was extended by replacing the four outermost d exponents by five and by adding four f functions, yielding a (17s, 13p, 10d, 4f) basis. The d and f functions were ANO contracted giving a [8s, 7p, 5d, 2f] contracted basis. This basis set gives a splitting between the $^1S(d^{10})$ and the $^3D(d^9s)$ states of 0.93 eV including relativistic effects and valence correlation, to be compared to the experimental value of 0.95 eV. For carbon a primitive (13s, 8p, 6d) basis[28] was used, ANO contracted to [4s, 3p, 2d]. For the active hydrogen a primitive (7s, 4p) basis contracted to [4s, 3p][29] was used. The inactive methyl hydrogens were described by the [3s, 1p] contracted basis used for the active hydrogen in the standard basis set described above.

(25) Blomberg, M. R. A.; Wahlgren, U. *Chem. Phys. Lett.* **1988**, *145*, 393.
(26) Huzinaga, S. *J. Chem. Phys.* **1965**, *42*, 1293.
(27) Bauschlicher, C. W., Jr.; Siegbahn, P.; Pettersson, L. G. M. *Theor. Chim. Acta* **1988**, *74*, 479.
(28) van Duijneveldt, F. B. IBM Research Report No. RJ 945 (1971).
(29) Chong, D. P.; Langhoff, S. R. *J. Chem. Phys.* **1986**, *84*, 5606.
(30) Martin, R. L.; Hay, P. J. *J. Chem. Phys.* **1981**, *75*, 4539.

Valence Bonds in the Main Group Elements. Generalized Valence Bond Description

Richard P. Messmer†

Contribution from the Research and Development Center, General Electric Company, Schenectady, New York 12301, and the Department of Physics, University of Pennsylvania, Philadelphia, Pennsylvania 19104. *Received May 30, 1989*

Abstract: The generalized valence bond (GVB) theory provides an ideal framework to test ideas regarding bonding in hypervalent molecules as it provides the *most general* orbital picture and at the same time it provides *unique orbitals*. However, it is very difficult to implement computationally and as a consequence the results presented here employ the usual strong orthogonality and perfect-pairing (SOPP) restrictions. Nonetheless the method is a substantial improvement beyond Hartree-Fock theory and provides a new perspective on back-bonding, participation of d-orbitals, multiple bonds, and the validity of the Octet rule. The ONF_3 and OPF_3 molecules are studied and the NO bond in the former is found to be composed of a single bond and *three back-bonds*, while the OP bond of the latter is a *triple bond*. Some general deductions regarding the nature of the bonding description in the full GVB method are made, leading to the qualitative scheme for discussing bonding which is applied to several examples.

Introduction

Much of the theoretical understanding of the chemical bond, both qualitative and quantitative, is based on the use of a single set of valence s, p, and d atomic orbitals at each atomic site in a molecule.[1] The concepts of π-bonds and δ-bonds arise from considering the interaction of atomic p or d orbitals, respectively, on adjoining atoms. The concept of hybrid orbitals makes use of linear combinations among a single set of valence atomic s, p, and d orbitals at a given nuclear site. The *linear combination of atomic orbitals* (LCAO) approximation forms the basis of modern computational quantum chemistry, whether the approach is semiempirical molecular orbital theory,[2] ab initio molecular orbital theory,[3] ab initio valence bond theory,[4] or more general approaches such as configuration interaction (CI) or multiconfiguration self consistent field (MCSCF).[5] Even in the ab initio

† Address correspondence to the author at the General Electric Company.

(1) (a) Pauling, L. *J. Am. Chem. Soc.* **1931**, *53*, 1367. Pauling, L. *The Nature of the Chemical Bond*; Cornell University Press: Ithaca, NY; 2nd ed., 1940; 3rd ed., 1960. (b) The vast literature that exists which subsequently developed and employed these ideas cannot be done justice here.
(2) Hoffmann, R.; Lipscomb, W. N. *J. Chem. Phys.* **1962**, *36*, 2179. Hoffmann, R. *J. Chem. Phys.* **1962**, *39*, 1397. Pople, J. A.; Beveridge, D. L. *Approximate Molecular Orbital Theory*; McGraw-Hill: New York, 1970. Baird, N. C.; Dewar, M. J. S. *J. Chem. Phys.* **1969**, *50*, 1262.
(3) Roothaan, C. C. J. *Rev. Mod. Phys.* **1951**, *23*, 69. Hall, G. G. *Proc. R. Soc. (London)* **1951**, *23*, 541. Pople, J. A. In *Modern Theoretical Chemistry*; Schaefer, H. F., III, Ed.; Plenum Press: New York, 1977; Vol. 3, Chapter 1.

0002-7863/91/1513-433$02.50/0